Available online at www.sciencedirect.com
SCIENCE DIRECT
International Journal of Heat and Fluid Flow 27 (2006) 445–455
International Journal of HEAT AND FLUID FLOW
www.elsevier.com/locate/ijhff

Turbulence characteristics of natural-convection boundary layer in air along a vertical plate heated at high temperatures

Yasuo Hattori [a,*], Toshihiro Tsuji [b], Yasutaka Nagano [c], Nobukazu Tanaka [a]

[a] Fluid Science Sector, Central Research Institute of Electric Power Industry, 1646 Abiko, Abiko-shi, Chiba-ken 270-1194, Japan
[b] Department of Environmental Technology, Graduate School of Engineering, Nagoya Institute of Technology, Gokiso-cho, Showa-ku, Nagoya 466-8555, Japan
[c] Department of Mechanical Engineering, Nagoya Institute of Technology, Gokiso-cho, Showa-ku, Nagoya 466-8555, Japan

Received 8 July 2004; received in revised form 23 June 2005; accepted 22 November 2005
Available online 3 March 2006

Abstract

Turbulence characteristics of a natural-convection boundary layer in air along a vertical plate heated at high temperatures are experimentally investigated. Two-dimensional velocity vectors and instantaneous temperature in the boundary layer at a wall temperature up to 300 °C are measured using a particle image velocimetry and a cold wire. From the correlation between the local Nusselt number Nu_x and the local Grashof number Gr_x, it was found that heat transfer rates even for a wall temperature of 300 °C are well expressed by an empirical formula obtained for low wall temperature and the region of transition from laminar to turbulence does not change much with an increase in wall temperature. In addition, the profiles of turbulent quantities measured at a wall temperature of 300 °C resemble those observed at low wall temperatures, and thus the effects of high heat on the turbulent behavior in the boundary layer are quite small. The measured velocity vectors and the higher-order statistics, such as skewness and flatness factors of fluctuating velocities and temperature, also suggest that the structure of large-scale fluid motions in the outer layer of the natural-convection boundary layer, closely connected with turbulence generation, is maintained even under high wall temperature conditions.

Keywords: Natural convection; Turbulent flow; Convective heat transfer; Boundary layer; High temperature; Particle image velocimetry

1. Introduction

The turbulent natural-convection boundary layers induced around highly heated bodies are frequently encountered in engineering applications, e.g., the accurate comprehension of the heat transfer characteristics is useful for evaluating the heat removal capability of electric power systems (Siebers et al., 1985; Sakamoto et al., 2000) and for designing fireproof buildings (Yoshie, 1996). Also, through the experimental results obtained under a relatively small temperature difference, it was suggested that the turbulent energy production near the wall is probably controlled by a peculiar mechanism, i.e., the fluctuation of thermal energy is directly converted into turbulent kinetic energy in the velocity field through density fluctuation (Tsuji et al., 1991). It may be possible that the turbulent natural-convection boundary layer takes on different characteristics, if the wall temperature increases and fluid properties change significantly.

Nevertheless, research concerning the turbulent natural-convection boundary layer induced by a large temperature difference has been insufficient, because of the difficulty in obtaining credible experimental data on flow and thermal fields. To the authors' knowledge, there are only two papers (Siebers et al., 1985; Yoshie, 1996) on experiments about the turbulent natural-convection boundary layer in air along a vertical plate heated at high temperatures which is one of the typical buoyant flows. Siebers et al. (1985) conducted experiments at wall temperatures ranging from 60 to 520 °C and investigated the correlation between the

* Corresponding author. Tel.: +81 4 7182 1181; fax: +81 4 7184 7142.
E-mail address: yhattori@criepi.denken.or.jp (Y. Hattori).

0142-727X/$ - see front matter © 2006 Elsevier Inc. All rights reserved.
doi:10.1016/j.ijheatfluidflow.2005.11.007

Nomenclature

$F(u)$, $F(v)$, $F(t)$	flatness factors of u, v and t
Gr_x	local Grashof number, $g\beta\Delta T_w x^3/\nu^2$
g	gravitational acceleration (m/s^2)
h	heat transfer coefficient (W/m^2 K)
Nu_x	local Nusselt number, hx/λ
R	spatial-correlation coefficient
$S(u)$, $S(v)$, $S(t)$	skewness factors of u, v and t
T	temperature (°C, K)
t	temperature fluctuation (K)
U	streamwise velocity (m/s)
u	streamwise velocity fluctuation (m/s)
v	transverse velocity fluctuation (m/s)
w	spanwise velocity fluctuation (m/s)
x	vertical distance from leading edge of flat plate (m)
y	horizontal distance perpendicular to flat plate (m)
z	spanwise distance from center line of flat plate (m)

Greeks

β	coefficient of volume expansion (1/K)
ΔT_w	temperature difference, $T_w - T_\infty$ (K)
δ_u	integral thickness of velocity boundary layer, $\int_0^\infty U/U_m \, dy$ (m)
δ_t	integral thickness of thermal boundary layer, $\int_0^\infty \theta \, dy$ (m)
λ	thermal conductivity (W/mK)
η	similarity variable for laminar boundary layer, $(y/x)Gr_x^{1/4}$
ν	kinematic viscosity (m^2/s)
θ	non-dimensional temperature, $(T - T_\infty)/\Delta T_w$

Subscripts

m	maximum value
w	wall condition
∞	ambient condition
(–)	time-averaged quantities

heat transfer rate and flow conditions. To account for variable properties effects on the heat transfer rate, they recommended the reference temperature method, and reported that the effect of high wall temperatures on heat transfer characteristics markedly appeared in the transition and turbulent regions, whereas the effect was not so obvious in the laminar region. However, information on the velocity field was not been reported, because their measurements were limited to the thermal field. Then, to obtain experimental data for verifying the capability of turbulence models, Yoshie (1996) measured the turbulent quantities in both velocity and temperature fields, such as standard deviations of velocity and temperature fluctuations, the Reynolds shear stress and turbulent heat fluxes, with a laser-Doppler velocimetry (LDV) system and a thermocouple (12 μm in diameter) at two different wall temperatures (59 and 429 °C). From these measurements, he suggested that the intensities of velocity fluctuations varied near a wall increased with wall temperature. However, his study did not identify turbulence structures in the boundary layer nor clarify how turbulent quantities changed as wall temperature increased, because the main objective of his study was the development of numerical simulation methods for boundary layer flows with high buoyancy. Thus, the exploration of the effect of high heat on the turbulence characteristics of the natural-convection boundary layers induced around high temperature bodies remains a very important subject of inquiry, and the accumulation of experimental data has been eagerly awaited to better understand the essential qualities of the boundary layer.

For the natural-convection boundary layer along a vertical plate heated at relative low wall temperatures, turbulent characteristics have been extensively investigated (Smith, 1972; Cheesewright and Doan, 1978; Cheesewright and Dastbaz, 1983; Kitamura et al., 1985; Tsuji and Nagano, 1988a,b, 1992). These studies indicated that the turbulence characteristics in the near-wall region of the natural-convection boundary layer along a vertical heated plate essentially differ from those of forced convection, e.g., Reynolds shear stress is not necessarily negative but almost zero in spite of the positive mean velocity gradient; quasi-coherent structures such as the low- and high-speed streaks and intermittent bursts seen in forced convection cannot be clearly recognized. In addition, through the measurements of turbulence statistics, it was found that such peculiar characteristics exist in the natural-convection boundary layer, regardless of wall temperature at $T_w < 100$ °C. Multi-point simultaneous measurements of the thermal field with several thermocouples (Cheesewright and Doan, 1978; Cheesewright and Dastbaz, 1983; Tsuji et al., 1992) and visualizations of the velocity field (Kitamura et al., 1985) also revealed a fundamental difference between the turbulence structures of the natural- and forced-convection boundary layers. In particular, a large eddy structure appeared in the outer layer strongly connected with the generation of turbulent energy and dominated the turbulence behavior for most of the boundary layer. (Here, we refer to the region from the wall to the maximum velocity location as the inner layer, and the region between the maximum velocity location and the edge of the boundary layer as the outer layer.)

The objective of the present study is to clarify the turbulent behavior of the natural-convection boundary layer in air along a vertical plate heated at high temperatures. The instantaneous velocity vectors and temperature in the boundary layer have been measured with a particle

image velocimetry (PIV) and a cold wire at various wall temperatures ranging from 90 to 300 °C. To firmly grasp the critical Grashof number of transitions from laminar to turbulence under high temperature conditions, the development of the thermal field in the boundary layer is initially investigated. Then, on the basis of the measured turbulent quantities, including higher-order statistics such as skewness and flatness factors, the effects of the wall temperature on the turbulence characteristics of the boundary layer are discussed, and the spatial-correlation coefficients for velocity fluctuations are also examined to clearly specify the variation in turbulence structure with increasing wall temperature.

2. Experimental apparatus and procedure

A schematic of the experimental apparatus is shown in Fig. 1. The apparatus used in the present study was designed to be applicable to experiments for natural-, combined- and forced-convection boundary layers and has been mainly used to examine combined-convection boundary layers. Since the details of the apparatus were presented in our previous reports (Hattori et al., 2000; Hattori, 2001), the specifications for the natural-convection experiments are described as follows. Fig. 2 shows the schematics of a front and a cross-section of the heated surface. The heated surface composed of an aluminum plate (4 m high, 0.8 m wide and 0.02 m thick), heat-insulating materials, and electric heaters was placed vertically in the test section of a vertical wind tunnel. To minimize the heat loss by radiation, the plate surface was polished to a mirror finish. A total of 20 electric heaters made of four sheath Nichrom wires were horizontally attached to the backside of the plate with cement and binding metals. The maximum output of each heater was 4 kW, and the surface temperature of the plate could be increased to about 500 °C. The surface temperature, monitored with 48 K-type sheath thermocouples, was kept uniform by controlling the heating current of each heater with digital indicating controllers and thirstier regulators.

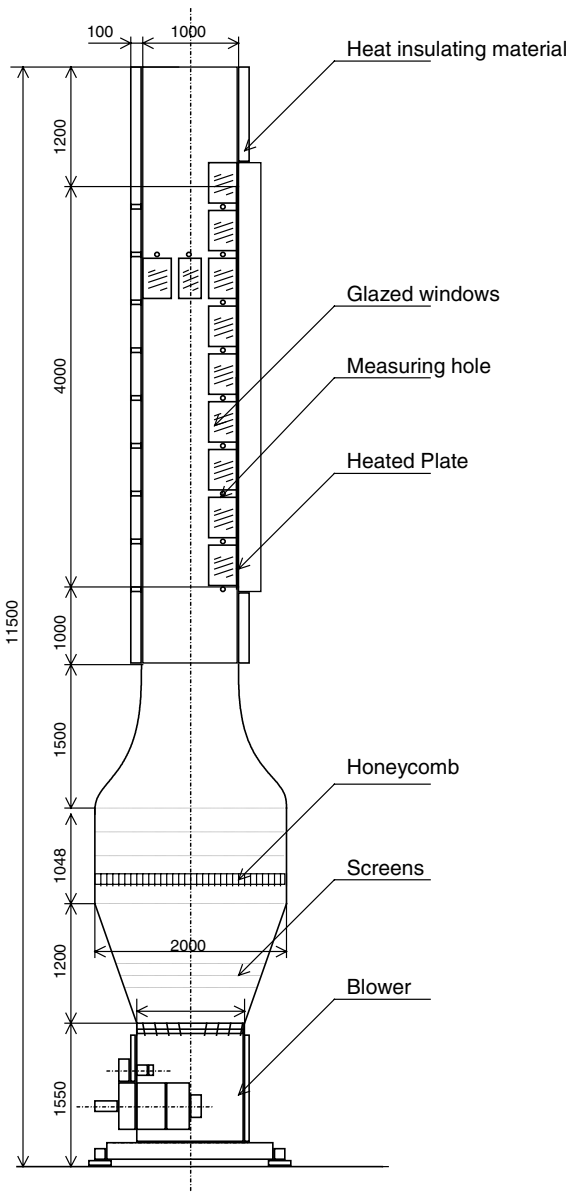

Fig. 1. Schematic of the experimental apparatus.

Two kinds of measurements for the boundary layer flow were carried out. One was a cold-wire measurement and the other a PIV measurement. The cold wire used to measure instantaneous temperature in the boundary layer including the near-wall region was 3.1 μm diameter tungsten, and its sensitive length was 4 mm. For the amplified temperature signals, the analog- to digital-conversion was performed at a sampling frequency of 500 Hz, and the instantaneous temperature was determined with digital processing on a workstation. Then, the statistics were calculated with about 4 min data for each measuring point.

The two-dimensional velocity field was measured with a PIV technique. The boundary layer flow was seeded with olive-oil mists as tracer particles illuminated by light sheets (about 1 mm in thickness) discharged from a double pulse Nd:YAG laser (90 mJ/pulse) system. The particle motions were captured by a CCD camera (1 k × 1 k pixels) with an 85 mm f/2.0 lens. The flow fields were visualized in the (x–y) plane perpendicular to the flat plate and in the (x–z) plane parallel to the flat plate. The distances between the lens and the object plane were approximately 0.7 m and 1.1 m for the measurements in the (x–y) and (x–z) planes, respectively. The physical sizes of the measuring areas in the (x–y) and (x–z) planes were 72×71 mm^{2}and 113×111 mm^2, respectively. The time interval between the two-pulsed illuminations was set at 400 μs [for the (x–y) plane measurement] and 500 μs [for the (x–z) plane measurement], so that the maximum displacement of successive particle images became approximately 10 pixels on the image plane. Visualized images captured by camera were directly stored into a PC hard disk as bmp files at 10 frames per second, and the local displacements of particle images were calculated using a cross-correlation method (Raffel et al., 1998) with interrogation windows of a size of

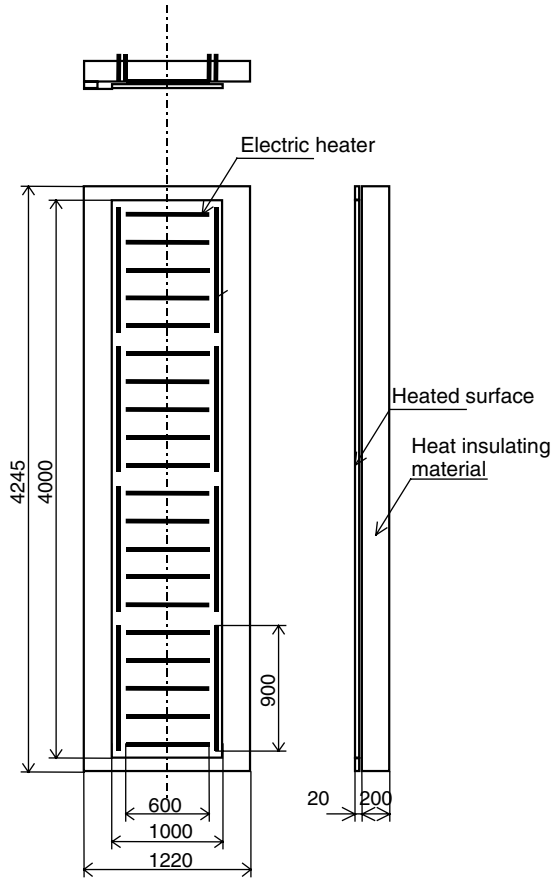

Fig. 2. Schematics of a front and a cross-section of the heated surface.

32×32 pixels. The sub-pixel algorithm on the assumption of a Gaussian profile for the spatial correlation was also applied to improve the dynamic spatial range of velocity vectors. About 2500 velocity vectors were obtained in each pair of images. After calculating velocity vectors, incorrect velocity vectors were removed with a median filter (Raffel et al., 1998), and empty data grids were filled with interpolated velocity vectors. Then, turbulence statistics were calculated from velocity vectors obtained with about 1000 images.

In preliminary experiments, flow and thermal conditions in the test section were verified. The uniformity of the surface temperature was within ±5 °C even at $T_w = 300$ °C. The heat loss by radiation from the heated surface and the conduction through heat-insulating materials was estimated to be approximately 15% of the electric power supplied to the plate for $T_w = 300$ °C. The accuracy of measurement was also demonstrated in the preliminary experiments. The experiments with a hot- and cold-wires and with a PIV were conducted for the natural-convection boundary layer at a relatively low wall temperature ($T_w = 60$ °C), and it was confirmed that the results for the mean velocity, the intensities of velocity fluctuations and the Reynolds shear stress obtained with the PIV agreed excellently with the hot- and cold-wire measurements, except $\eta < 1$, i.e., the estimated uncertainties (95% coverage) were 8% for U at maximum mean velocity location. Also, from the frequency spectra of measured velocity fluctuations, it was assured that the PIV could well capture fluctuations dominant in the turbulent natural-convection boundary (Tsuji et al., 1992). It is well known that the error in velocity measurements with a PIV is caused by the large velocity gradient, especially in the near-wall region of turbulent forced-convection boundary layer. But, the velocity gradient of natural convection is quite smaller than that of forced convection, and the effects of velocity gradient on the cross-correlation coefficient under the present experimental conditions. Consequently, the PIV measurement for the velocity field was judged to be reasonable, although small-scale structures related to high-frequency fluctuations could not be discussed. As to the temperature measurement, the example of profile of measured mean temperature in the near-wall region, which was used for the estimation of local heat transfer rate, is demonstrated in Fig. 3. The mean temperature profile can be approximated to a straight line, assuring that the present measurements were highly accurate (Tsuji and Nagano, 1988b).

The experiments were carried out under the condition of constant and uniform wall temperatures ($T_w = 90$–300 °C). The ambient fluid temperature T_∞ was somewhat different for each experiment, in the range of 20–30 °C. The cold-wire measurement was conducted in the vertical center-plane of the test section. To examine the development of the boundary layer, the vertical distance x from the leading edge of the flat plate to the measuring locations changed from 0.265 m to 3.265 m. In the PIV measurement, the CCD camera was fixed at $x = 2.965$ m to observe turbulence behavior.

As the temperature difference between the wall and ambient increases, the variable property effects on the normalization of experimental data become significant, so that some reference temperature methods have been recommended. For the variable properties effects on the heat transfer rates in the turbulent natural-convection boundary layer, Siebers et al. (1985) indicated that the heat transfer

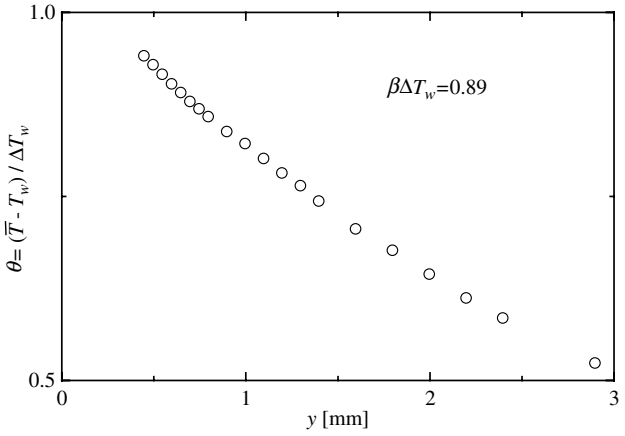

Fig. 3. Example of profile of measured mean temperature in the near-wall region.

rates were well correlated by employing all the properties evaluated at the ambient temperature and a wall-to-ambient temperature ratio correction. In the present study, however, physical properties were evaluated at the film temperature T_f [$=(T_w + T_\infty)/2$] except for the coefficient of volume expansion β ($=1/T_\infty$) to demonstrate the experimental results of heat transfer rates and turbulent statistics as presented later. Thus, the local Grashof numbers Gr_x ranged from 1.91×10^8 to 3.51×10^{11}, and the dimensionless temperature differences $\beta\Delta T_w$ [$=\beta(T_w - T_\infty)$] equaled 0.2 at $T_w = 90$ °C and 0.9 at $T_w = 300$ °C.

3. Results and discussion

3.1. Development of boundary layer

The experimental results of the heat transfer rate h for various $\beta\Delta T_w$ values, estimated from temperature gradients near the wall measured with a cold wire, are shown in Fig. 4 in the relationship between Nu_x and Gr_x. In the figure, the solid and dotted lines represent the empirical equations for laminar flow and turbulent, respectively, which were obtained in the experiment of Tsuji and Nagano (1988a) under the condition of small $\beta\Delta T_w$ values ($T_w = 60$, 100 °C). The heat transfer rates are well correlated even for $\beta\Delta T_w = 0.9$ with the empirical equations, and the differences in Nu_x between the measurements and empirical equations are within 5%. It should be emphasized that the transition region from laminar flow to turbulence does not change much with $\beta\Delta T_w$ values, and thus the transition Grashof number for $\beta\Delta T_w = 0.9$ is roughly equal to that for $\beta\Delta T_w = 0.2$.

For $\beta\Delta T_w = 0.89$, the temperature profiles of mean and fluctuation intensity in the development of the boundary layer are shown in Fig. 5. Since it has been reported that the turbulence statistics near the wall in the turbulent boundary layer are well correlated with the similarity variables used for the laminar natural-convection boundary

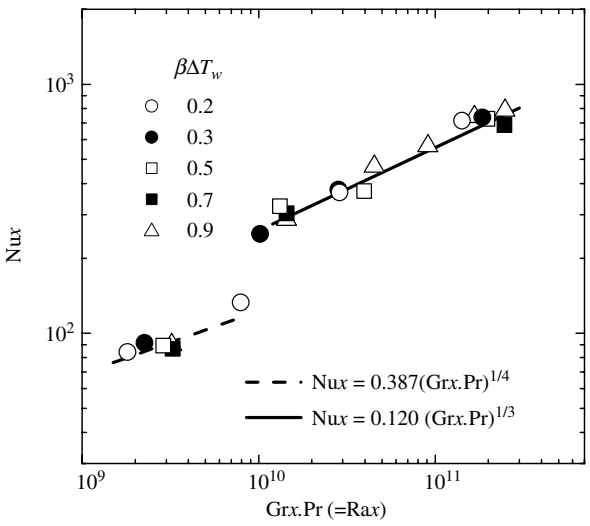

Fig. 4. Heat transfer rate for various values of $\beta\Delta T_w$.

layer (Tsuji and Nagano, 1989), the profiles are normalized with these similarity variables. In the present study, the temperatures at the wall and ambient are almost constant in the measurement, so that the value of Gr_x increases consistently with x. At $Gr_x = 1.91 \times 10^8$, the laminar boundary layer forms along the plate, and the intensity of temperature fluctuation is almost zero. When the boundary layer changes from laminar flow to transition with an increase in Gr_x, the temperature fluctuation becomes quite large, and so the maximum value of the dimensionless fluctuation intensity reaches 0.15 at $Gr_x = 4.54 \times 10^9$. Simultaneously, the mean temperature profile begins to change, and the boundary layer broadens abruptly. With a further increase in Gr_x, the boundary layer grows to turbulence, and these profiles are similar to those measured at relatively low wall temperatures (Tsuji and Nagano, 1988a,b).

The change in waveforms of the temperature fluctuation t observed for $\beta\Delta T_w = 0.89$ and $Gr_x = 1.91 \times 10^8$–3.51×10^{11}, which are normalized by the relevant fluctuation intensities, is displayed in Fig. 6. Obviously, the fluctuation in the laminar boundary layer for $Gr_x = 1.91 \times 10^8$ is extremely small. As Gr_x increases, harmonic waves with a specific frequency of about 12 Hz appear at $Gr_x = 4.54 \times 10^9$. This Gr_x value provides the beginning of change in the temperature profiles of mean and fluctuation intensity as shown in Fig. 5. As suggested by Polymeropoulos and Gebart (1967), Dring and Gebart (1969), such harmonic waves characterize the occurrence of transition from laminar to turbulence in the natural-convection boundary layer. When Gr_x further increases, the turbulent boundary layer develops along the plate and long-period waves due to large-scale fluid motion become dominant in the temperature fluctuation.

These results indicate that the transition to turbulence of the boundary layer occurs at $Gr_x = 10^9$–10^{10}, even for $\beta\Delta T_w = 0.89$. This critical Grashof number agrees well with that at relatively low wall temperatures ($Gr_x = 1.1 \times 10^9$–9.9×10^9 for $T_w = 60$, 100 °C) obtained by Tsuji and Nagano (1988a). On the other hand, Siebers et al. (1985) suggested that the critical Grashof number suddenly decreases with an increase in wall temperature. This noticeable discrepancy between both results may be caused by a difference in the experimental conditions, especially in the magnitude of disturbances included in the ambient fluid, because the transition of the boundary layer strongly depends on it (Schlichting, 1979). In the measurement of Siebers et al., a wind tunnel horizontally placed in open-air was used chiefly to examine the combined convection driven by orthogonal buoyant and inertia forces. Thus, quite large disturbances were probably involved in the test section. In the present study, a vertical wind tunnel was used, and disturbances in the test section were suppressed to the lowest possible level.

3.2. Basic turbulence statistics

For $T_w = 300$ °C ($\beta\Delta T_w = 0.89$), the turbulence statistics were measured with a PIV and a cold wire at $x =$

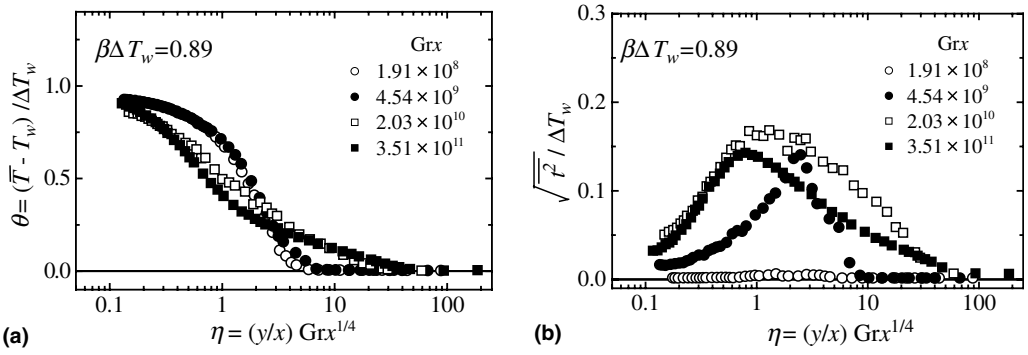

Fig. 5. Change in temperature profiles for mean and fluctuation intensity with development of boundary layer for $\beta\Delta T_w = 0.89$. (a) Mean temperature profiles and (b) intensity of temperature fluctuation.

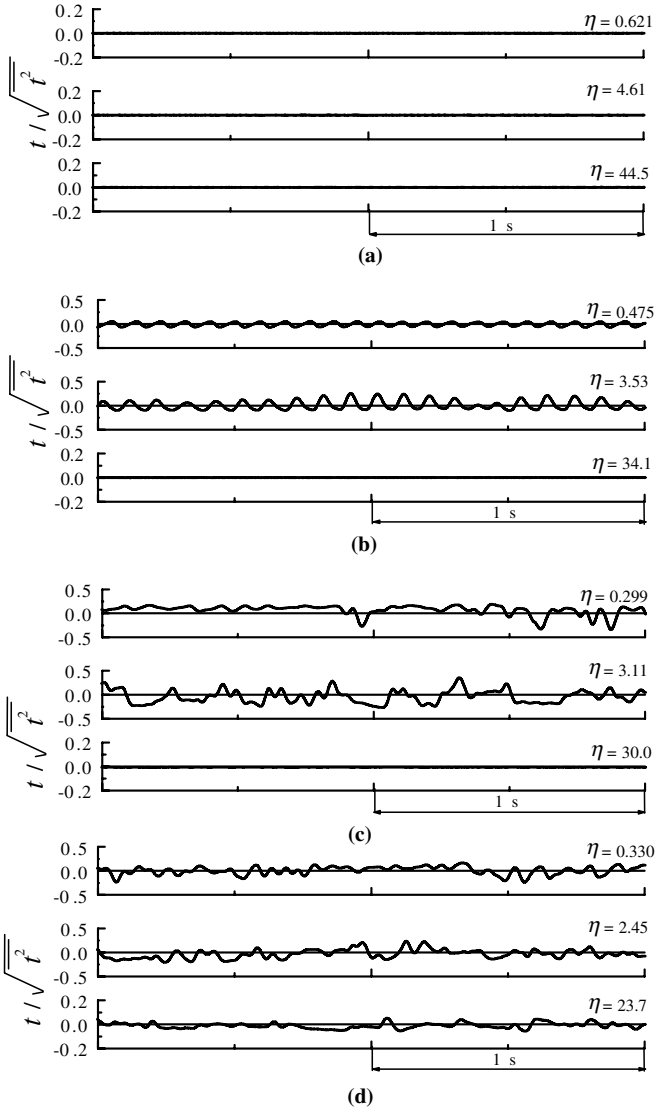

Fig. 6. Change in waveform of temperature fluctuation with development of boundary layer for $\beta\Delta T_w = 0.89$. (a) $Gr_x = 1.91 \times 10^8$, (b) $Gr_x = 4.54 \times 10^8$, (c) $Gr_x = 2.03 \times 10^{10}$ and (d) $Gr_x = 3.51 \times 10^{11}$.

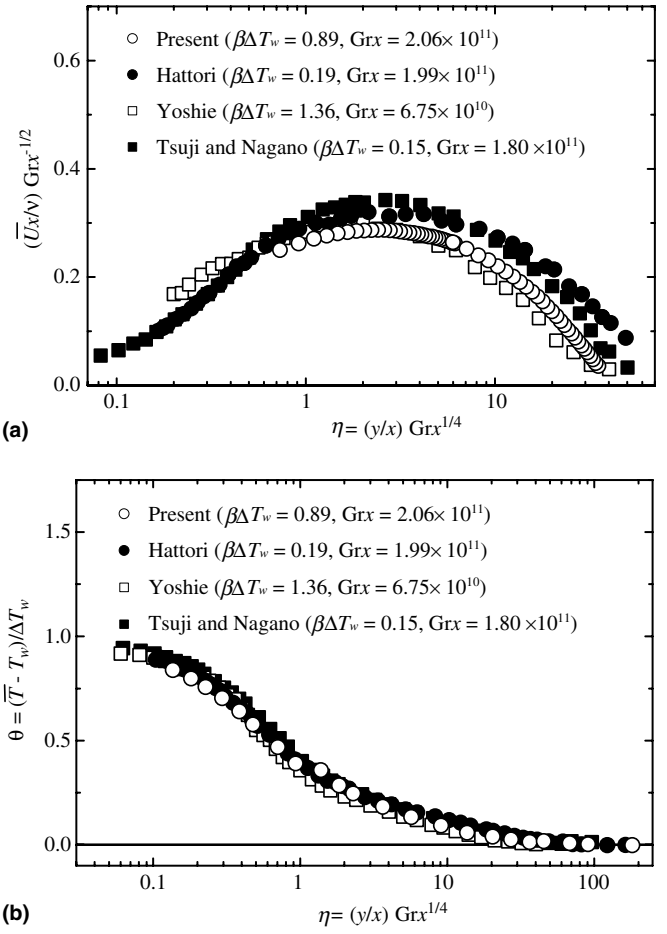

Fig. 7. Mean velocity and temperature profiles. (a) Mean velocity profile and (b) mean temperature profile.

2.965 m ($Gr_x = 2.06 \times 10^{11}$). Streamwise mean velocity and mean temperature profiles are shown in Fig. 7. These profiles were normalized by the similarity variable for the laminar natural-convection boundary (Tsuji and Nagano, 1989). Also shown in these figures are experimental results of Yoshie (1996) for $\beta\Delta T_w = 1.36$ and $Gr_x = 6.75 \times 10^{10}$ with a LDA system and thermocouples, and hot- and cold-wire measurements of Hattori (2001) for $\beta\Delta T_w = 0.19$ and $Gr_x = 1.99 \times 10^{11}$ and Tsuji and Nagano (1988a,b) for $\beta\Delta T_w = 0.15$ and $Gr_x = 1.80 \times 10^{11}$. As seen in the figures,

despite the $\beta\Delta T_w$ values, there is general agreement among these profiles, although quantitative discrepancies exist in the maximum mean velocity and boundary layer thickness.

Fig. 8 presents the intensity profiles of streamwise and transverse velocity fluctuations, u and v, and temperature fluctuation t. The profile of the Reynolds shear stress $\overline{uv}$ is shown in Fig. 9. These profiles are normalized with the maximum mean velocity $\overline{U}_m$ and temperature difference ΔT_w. For comparison, the data of Yoshie (1996), Hattori (2001) and Tsuji and Nagano (1988a,b) are also shown in the figures. The intensities of velocity fluctuations, u and v, and temperature fluctuations agree well with those obtained by Tsuji and Nagano (1988a,b) and Hattori (2001) under low wall temperature conditions for most of the boundary layer, and the maximum intensities of velocity fluctuations, u and v, occur in the outer layer beyond the maximum mean velocity location, while the maximum intensity of temperature fluctuation is observed in the near-wall region of the inner layer. The Reynolds shear stress $\overline{uv}$ becomes positive near the maximum mean velocity location and almost zero in the inner layer as shown in Fig. 9. This profile is very close to that of Tsuji and Nagano (1988b), in which reliability was confirmed by comparing the indirect measurements estimated from the integral equation for momentum transfer.

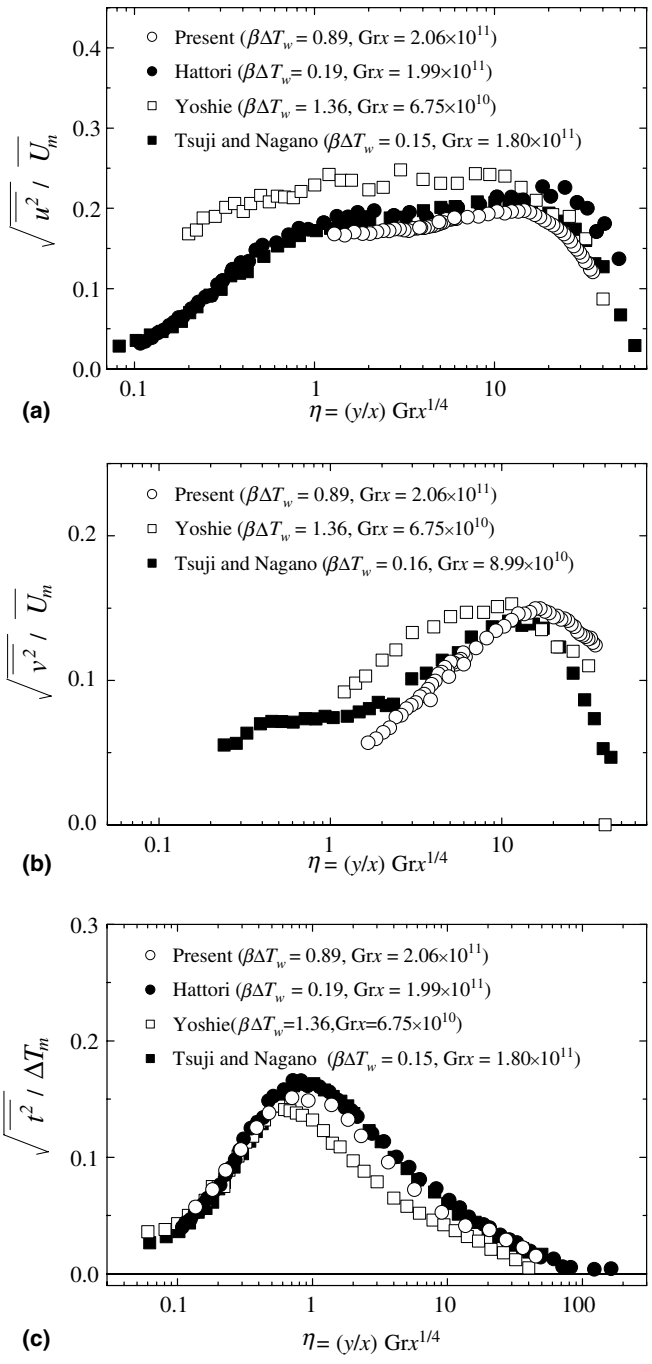

Fig. 8. Intensity of velocity and temperature fluctuations. (a) Intensity of streamwise velocity fluctuation u, (b) intensity of transverse velocity fluctuation v and (c) intensity of temperature fluctuation t.

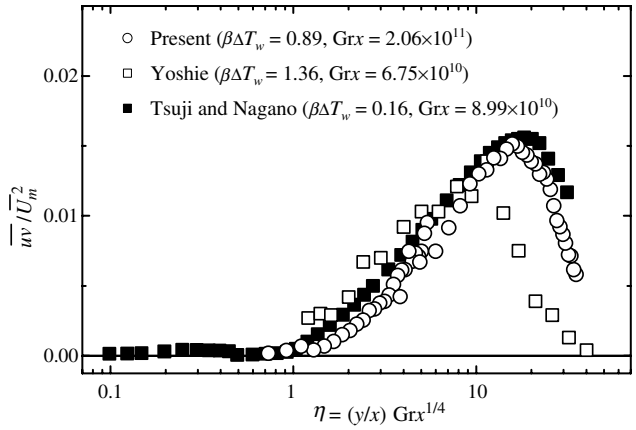

Fig. 9. Reynolds shear stress.

These statistics on the turbulent natural-convection boundary layer are indeed peculiar to the turbulent natural-convection boundary layer (Tsuji and Nagano, 1988a,b; Ampofo and Karayiannis, 2003). In particular, the profile of $\overline{uv}$, which becomes almost zero in the inner layer of natural-convection boundary layer, indicates that the turbulence generation near the wall of natural-convection boundary layer does not directly connect with the Reynolds shear stress and the mean velocity gradient. Such peculiar profiles of turbulent quantities observed under the condition of low temperature differences appear even in the boundary layer for $\beta\Delta T_w = 0.89$. Thus, the effects of $\beta\Delta T_w$ on the profile measurements are quite small and similar profiles appear regardless of the $\beta\Delta T_w$ values.

3.3. Structural characteristics

For $\beta\Delta T_w = 0.89$, the skewness and the flatness factors of velocity and temperature fluctuations in the turbulent boundary layer at $Gr_x = 2.06 \times 10^{11}$ are presented in Fig. 10. Here, the distance from the wall y is normalized by the integral thicknesses of the velocity and thermal boundary layers (Tsuji and Nagano, 1989). These factors differ somewhat from those for a Gaussian distribution.

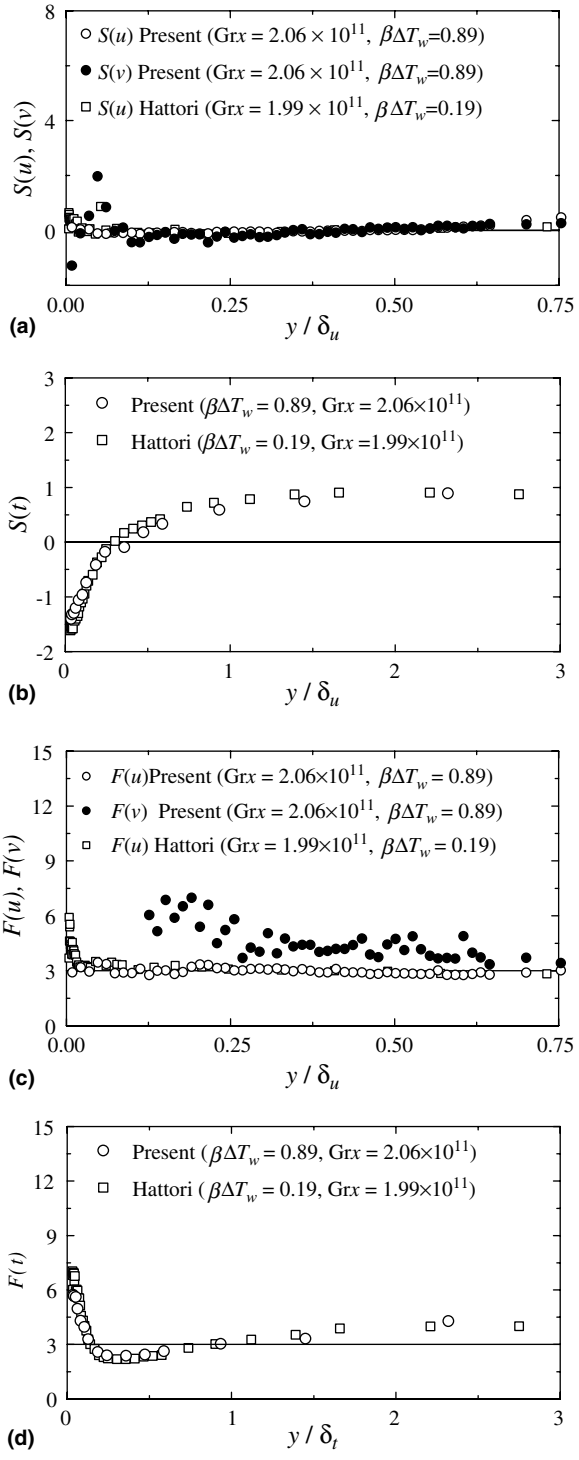

Fig. 10. Skewness and flatness factors of velocity and temperature fluctuations. (a) Skewness of velocity fluctuations u and v, (b) skewness of temperature fluctuation t, (c) flatness of velocity fluctuations u and v and (d) flatness of temperature fluctuation t.

The skewness factor $S(u)$ becomes positive in the near-wall and outer layers and takes slightly negative values around the maximum mean velocity location ($y/\delta_u = 0.1$), while the flatness factor $F(u)$ in the near-wall region substantially exceeds the value of 3. The flatness factor $F(v)$ takes positive values larger than $F(u)$ and $F(t)$ in the whole boundary layer region, so that velocity fluctuation v is more intermittent. On the other hand, the skewness factor $S(t)$ becomes negative near the wall and positive in the outer layer (the maximum mean velocity location corresponds to $y/\delta_t = 0.65$), and the profile of the flatness factor $F(t)$ is roughly similar to that of $F(u)$. These profiles of skewness and flatness factors are associated with large-scale structures, which are peculiar to the turbulent natural-convection boundary layer (Tsuji et al., 1992; Tsuji and Nagano, 1988a,b). To discuss the dependence of the higher-order statistics on T_w, the skewness flatness factors of u and t measured with cold and hot wires for $\beta\Delta T_w = 0.19$ and $Gr_x = 1.99 \times 10^{11}$ (Hattori, 2001) are also shown for reference in Fig. 10. Despite the marked difference in $\beta\Delta T_w$, the profiles are unaltered. Also, for the turbulent natural-convection boundary layer flow in a square cavity, similar profiles of skewness and flatness factors of temperature fluctuations were obtained with a 2D LDA and a thermocouple (Tian and Karayiannis, 2000), and thus the wall temperature T_w has only a limited influence on the higher-order statistics closely related to the structural characteristics of the boundary layer.

For $\beta\Delta T_w = 0.89$ and $Gr_x = 2.06 \times 10^{11}$, the transverse- and spanwise-correlation coefficients of velocity fluctuations are shown in Fig. 11, compared with those obtained with a PIV measurement for $\beta\Delta T_w = 0.19$ and $Gr_x = 1.77 \times 10^{11}$ (Hattori, 2001). The fixed point to calculate the spatial-correlation coefficients is located at the maximum mean velocity. Though the characteristics of

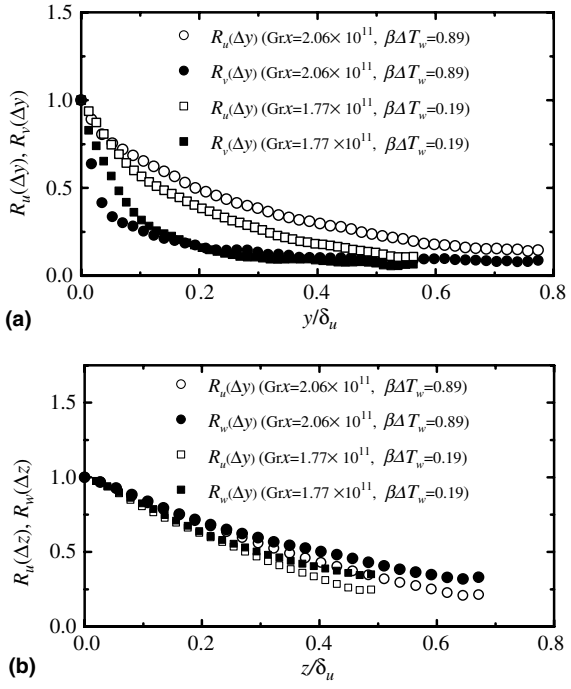

Fig. 11. Spatial correlation coefficient of velocity fluctuations. (a) Transverse-spatial correlation coefficient of u and v and (b) spanwise-spatial correlation coefficient of u and w.

the profiles are independent of $\beta\Delta T_w$, there is a quantitative discrepancy between $R_u(\Delta y)$ and $R_v(\Delta y)$. With increasing two-point separation, the value of $R_v(\Delta y)$ decays more rapidly than that of $R_u(\Delta y)$. On the other hand, there is an overall similarity between the spatial correlations of u and w in the z direction. The integral scale obtained from the $R_u(\Delta y)$ profile, regarded as a characteristic length related to the large-scale structure, was estimated at about 0.3 when normalized by the integral thickness of the velocity boundary layer. This value agrees well with that obtained from the experiment for the small $\beta\Delta T_w$ (Tsuji et al., 1992).

The distributions of two-point spatial correlation coefficients for u and v in the $(x–y)$ plane and for u and w in the $(x–z)$ plane are presented in Fig. 12. These correlation coefficients are obtained for the fixed point located at the maximum mean velocity location in the $(x–y)$ plan and at $y/\delta_u = 1$ in the $(x–z)$ plane, so as to observe fluid motions in the region from the maximum mean velocity location to the edge of the boundary layer. The distribution of spatial correlation for u in the $(x–y)$ plane is elongated in the x direction and is inclined at a small angle to the wall as seen in Fig. 12(a), which indicates an inactive propagation of fluid motions in the y direction. The inclination of contour

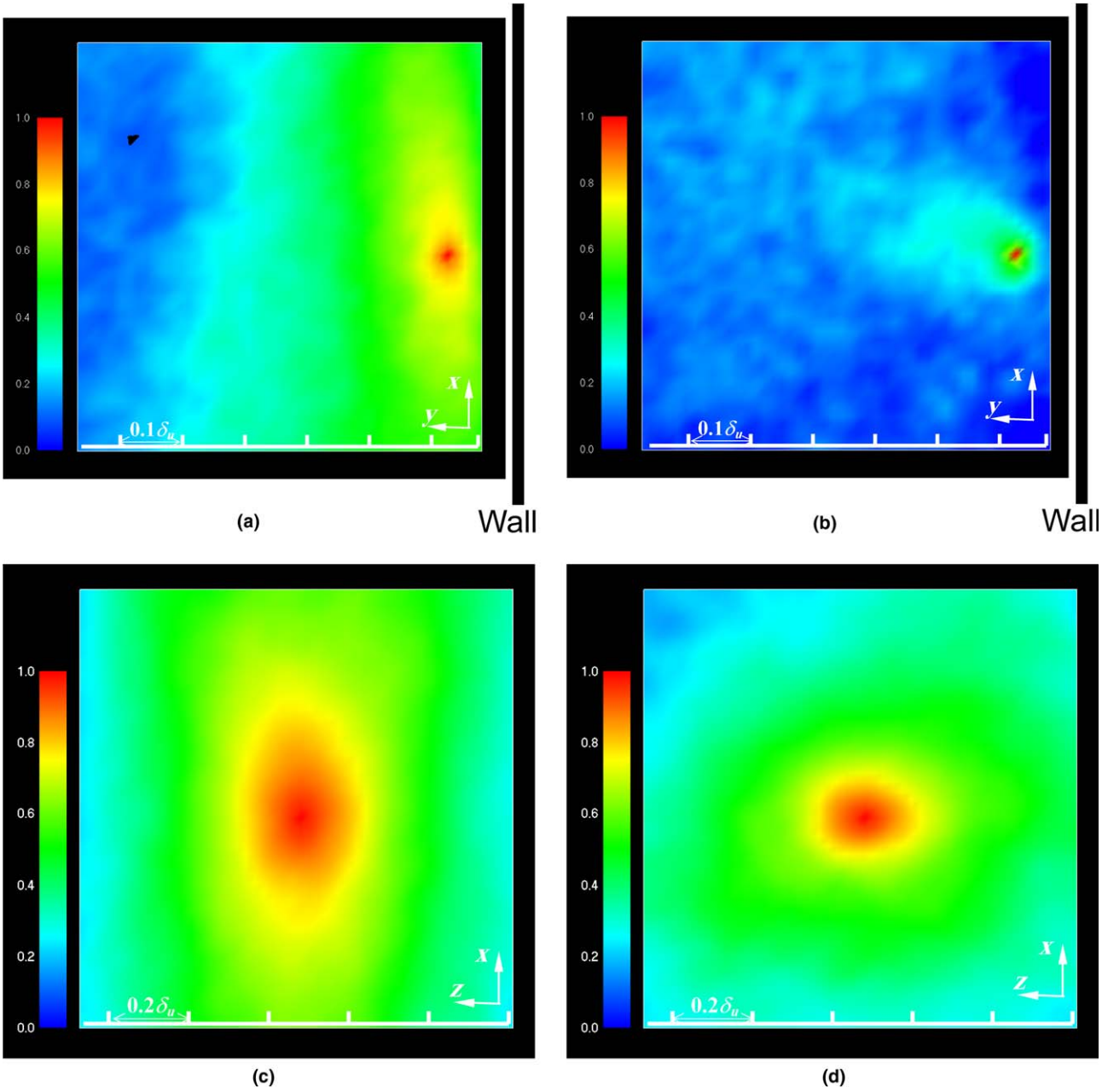

Fig. 12. Distributions of spatial correlation coefficients in $(x–y)$ and $(x–z)$ planes. (a) Streamwise velocity fluctuation u in $(x–y)$ plane, (b) transverse velocity fluctuation v in $(x–y)$ plane, (c) streamwise velocity fluctuation u in $(x–z)$ plane and (d) spanwise velocity fluctuation w in $(x–z)$ plane.

defined as the angle between the ridgeline and the wall has been used to define the orientation of dominant flow structures. The average angle estimated from the contour is about 7° and this value is approximately identical to that for forced convection (Liu et al., 2001). On the other hand, it was reported that the contour of spatial-correlation coefficients for temperature fluctuation in the thermal-field of natural-convection had a different value of inclination (=15–20°) (Cheesewright and Dastbaz, 1983). This fact indicates a poor relation between the structures in the velocity and thermal fields of the natural-convection boundary layer. As shown in the figure, high values of correlation coefficients for u fluctuation also appear in the inner layer. This implies that the large-scale fluid motions have an effect on the structure very near the wall. In contrast to u, the contour of correlation coefficient for v, as shown in Fig. 12(b), rapidly shrinks with an increase in the spacing between two points, which indicates that the scale of v is quite small. The shapes of these contours are close to that was observed in the forced-convection boundary layer. Thus, near the maximum mean velocity location in the natural convection, the structure of the velocity field seems to be fairly similar to that for forced convection.

In the (x–z) plane, the scale of u in the x direction is larger than that in the z direction (Fig. 12(c)), while the scales of w in each direction become almost identical (Fig. 12(d)), indicating the significant anisotropy of the large-scale structure in the outer layer. This contour is significantly different from that for forced convection, i.e., the correlation contour for u fluctuation in the outer layer of natural convection becomes positive in the whole visualized region ($\cong\delta_u \times \delta_u$), while that for forced convection alters from positive to negative as the spacing between two points in the z direction increases. Thus, the streaky structure as observed in forced convection is not clearly detected in this boundary layer.

Fig. 13 illustrates an example of fluctuating velocity vectors consisting of u and v with instantaneous values of uv and vorticity observed in the (x–y) plane. It is observed in Fig. 13 that the winding of high momentum flows generates strong vorticies with scales beyond the thickness δ_u in the x direction. Also observed is the large-scale fluid moving at a high-speed ($u > 0$) toward the outer layer ($v > 0$), which is the important 'Q1 ($u > 0$, $v > 0$)' motion contributing to the Reynolds shear stress. Such a fluid motion may substantially contribute to the production of turbulent energy, because uv takes a large positive value, the mean velocity gradient is negative in the outer layer, and simultaneously vigorous vortices generate. Thus, it is confirmed that the large-scale structures involving the Q1 motions are directly related to the turbulence generation in the outer layer of the boundary layer.

Also, an example of the fluctuating velocity vectors, consisting of u and w with instantaneous vorticity observed at $y/\delta_u = 1$ in the (x–z) plane, is shown in Fig. 14. Here, it should be noted that these distributions were not captured at one time. In the (x–z) plane, flow windings in the velocity field due to low-speed fluid motions appear in the entire visualized region, and vortices are generated by the flow windings. The scales of such fluid motions correspond approximately to the boundary layer thickness, and strong vortices appear near the location where flow windings are observed.

Consequently, it was found that, regardless of wall temperature T_w, the large-scale structure entirely dominated the velocity field in the outer layer, and large-scale fluid

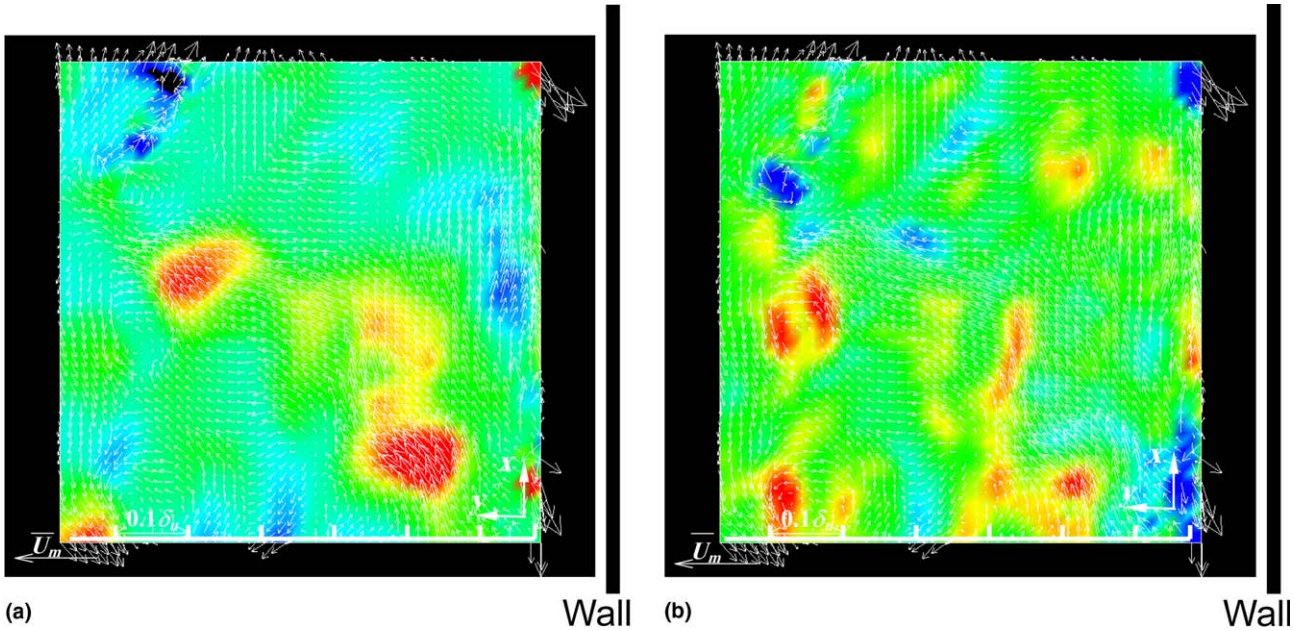

Fig. 13. Fluctuating velocity vectors in (x–y) plane of outer layer (a) with uv (b) with vorticity.

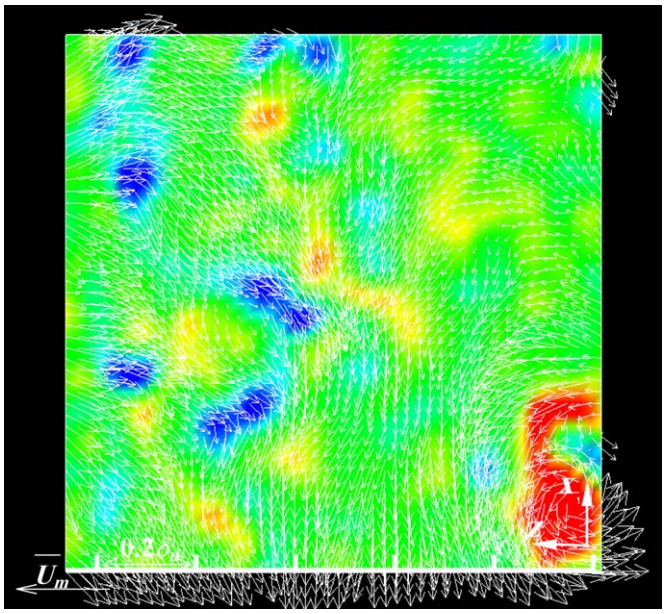

Fig. 14. Fluctuating velocity vectors with instantaneous vorticity observed at $y/\delta_u = 1$ in (x–z) plane.

motions mainly generated the turbulent kinetic energy sustaining the turbulent natural-convection boundary layer.

4. Conclusions

The turbulent natural-convection boundary layer in air along a vertical plate heated at high temperatures up to 300 °C has been measured using particle image velocimetry and a cold wire. The results obtained may be summarized as follows:

1. The heat transfer rates even for $\beta\Delta T_w = 0.9$ are well expressed with the empirical equations obtained by the experiments under the conditions of small $\beta\Delta T_w$ values. Moreover, the region of transition from laminar to turbulence does not change much with $\beta\Delta T_w$ values, and the critical Grashof number for $\beta\Delta T_w = 0.9$ is roughly equal to that for $\beta\Delta T_w = 0.2$.
2. The effects of a high heat on the structural characteristics of the turbulent boundary layer are quite small, and the profile measurements of turbulent quantities for $\beta\Delta T_w = 0.89$ preserve the appearances observed under the conditions of small $\beta\Delta T_w$ values. That is, despite a remarkable increase in the wall temperature, the maximum intensities of velocity fluctuations, u and v, occur in the outer layer, and the Reynolds shear stress uv becomes positive at the maximum mean velocity location and almost zero near the wall.
3. Wall temperature has only a limited effect on the higher-order statistics, so the changes in the profiles of skewness and flatness factors are quite small in spite of the substantial difference in $\beta\Delta T_w$.
4. Regardless of wall temperature, the large-scale structure corresponding to the boundary layer thickness entirely dominates the velocity field in the outer layer and closely relates to the generation of the turbulence kinetic energy.

References

Ampofo, F., Karayiannis, T.G., 2003. Experimental benchmark data for turbulent natural convection in an air filled square cavity. Int. J. Heat Mass Transfer 46, 3551–3572.

Cheesewright, R., Doan, K.S., 1978. Space–time correlation measurements in a turbulent natural convection boundary layer. Int. J. Heat Mass Transfer 21, 911–921.

Cheesewright, R., Dastbaz, A., 1983. The structure of turbulence in a natural convection boundary layer. In: Proc. 4th Turbulent Shear flow Symposium, pp. 17.25–17.30.

Dring, R.P., Gebart, B., 1969. An experimental investigation of disturbance amplification in external laminar natural convection flow. J. Fluid Mech. 36, 447–464.

Hattori, Y., 2001. Turbulent characteristics and transition behavior of combined-convection boundary layer along a vertical heated plate. Ph.D. thesis, Nagoya Institute of Technology.

Hattori, Y., Tsuji, T., Nagano, Y., Tanaka, N., 2000. Characteristics of turbulent combined-convection boundary layer along a vertical heated plate. Int. J. Heat Fluid Flow 21, 520–525.

Kitamura, K., Koike, M., Fukuoka, I., Saito, T., 1985. Large eddy structure and heat transfer of turbulent natural convection along a vertical flat plate. Int. J. Heat Mass Transfer 28, 837–850.

Liu, Z., Adrian, R.J., Hanratty, T.J., 2001. Large-scale modes of turbulent channel flow: transport and structure. J. Fluid Mech. 448, 53–80.

Polymeropoulos, C.E., Gebart, B., 1967. Incipient instability in free convection laminar boundary layers. J. Fluid Mech. 30, 225–239.

Raffel, M., Willert, E., Kompenhans, J., 1998. Particle Image Velocimetry. Springer-Verlag, Berlin, Heidelberg.

Sakamoto, K., Koga, T., Wataru, M., Hattori, Y., 2000. Heat removal characteristics of vault storage system with cross flow for spent fuel. Nucl. Eng. Des. 195, 57–68.

Schlichting, H., 1979. In: Boundary-Layer Theory. McGraw-Hill, New York, p. 572.

Siebers, D.L., Moffatt, R.F., Schwind, R.G., 1985. Experimental, variable properties natural convection from a large, vertical, flat plate. Trans. ASME J. Heat Transfer 107, 124–132.

Smith, R.R., 1972. Characteristics of turbulence in free convection flow past a vertical plate, Ph.D. thesis, University of London.

Tian, Y.S., Karayiannis, T.G., 2000. Low turbulence natural convection in an aire filled square cavity—Part II: the turbulence quantities. Int. J. Heat Mass Transfer 43, 867–884.

Tsuji, T., Nagano, Y., 1988a. Characteristics of a turbulent natural convection boundary layer along a vertical flat plate. Int. J. Heat Mass Transfer 31, 1723–1734.

Tsuji, T., Nagano, Y., 1988b. Turbulence measurements in a natural convection boundary layer along a vertical flat plate. Int. J. Heat Mass Transfer 31, 2101–2111.

Tsuji, T., Nagano, Y., 1989. Velocity and temperature measurements in a natural convection boundary layer along a vertical flat plate. Exp. Thermal Fluid Sci. 2, 208–215.

Tsuji, T., Nagano, Y., Tagawa, M., 1991. Thermally driven turbulent boundary layer. In: Proc. 8th Symp. Turbulent Shear Flows 2, pp. 24.3.1–24.3.6.

Tsuji, T., Nagano, Y., Tagawa, M., 1992. Experiment on spatio-temporal turbulent structures of a natural convection boundary layer. Trans. ASME J. Heat Transfer 114, 901–908.

Yoshie, R., 1996. Numerical simulation of variable density flow with high buoyancy, Ph.D. thesis, The University of Tokyo (in Japanese).